Hindawi
Journal of Food Quality
Volume 2020, Article ID 8844167, 11 pages
https://doi.org/10.1155/2020/8844167

Research Article

Study on Biodegradable Chitosan-Whey Protein-Based Film Containing Bionanocomposite TiO_2 and *Zataria multiflora* Essential Oil

Maryam Gohargani,[1] Hannan Lashkari ,[2] and Alireza Shirazinejad[1]

[1]*Department of Food Science and Technology, Sarvestan Branch, Islamic Azad University, Sarvestan, Iran*
[2]*Department of Food Science and Technology, Zarindasht Branch, Islamic Azad University, Zarindasht, Iran*

Correspondence should be addressed to Hannan Lashkari; hlashkari@gmail.com

Received 15 June 2020; Revised 28 August 2020; Accepted 31 August 2020; Published 15 September 2020

Academic Editor: Amin Mousavi Khaneghah

In our research, a composite film of whey protein isolate (WPI)/chitosan incorporated with TiO_2 nanoparticles (NPs) and essential oil of *Zataria multiflora* (ZEO) was developed. The resulting composite films were evaluated by FTIR, SEM, and XRD, and also the physicochemical characteristics including color, mechanical properties, swelling ratio, and water vapor permeability (WVP) were studied. SEM graphs exhibited that the samples had a uniform and homogeneous structure where TiO_2 NPs and ZEO were well dispersed. FTIR and XRD findings also show that the hydrogen bonds and hydrophobic interactions are the main interactions between the composite WPI/chitosan and TiO_2. The crystalline nature of the composite samples increased with the increase of NP content. Nevertheless, ZEO had an insignificant effect on the functional groups and the crystallinity of composite samples. The film visual characterization revealed that, by adding and increasing the TiO_2 and TiO_2-ZEO, sample lightness and opacity significantly increased. Additions of TiO_2 remarkably ($p < 0.05$) improved the water vapor and mechanical properties of composite samples, although the loading of ZEO, regardless of TiO_2 incorporation, led to a considerable decrement of these properties. Furthermore, composite films containing ZEO combined with 2% of TiO_2 compared with 1% of NPs blended with ZEO had strong antimicrobial properties against *Staphylococcus aureus*, *Escherichia coli*, and *Listeria monocytogenes*. Generally, the findings proposed that the addition of TiO_2 reinforces the properties of composite films with a synergistic effect of ZEO loading on the antibacterial ability, by which the resulting biodegradable composite samples can be used as a food active packaging material.

1. Introduction

Nowadays, the increase in the global concern of food quality and safety together with the environmental influences of nonbiodegradable plastic material wastes has led to the research and studies on the renewable and eco-friendly edible coating and films [1]. Biopolymers including proteins, lipids, polysaccharides, and their mixtures are considered as the main engaged materials for this purpose due to their benefits such as biodegradability, high availability, and renewability [2, 3]. Natural ingredients and essential oils extracted from plants are usually incorporated into the packaging ingredients to increase their mechanical and chemical properties and also prevent the packaged products from microbial activities and reduce the oxidation of lipids which can promote the quality of food products compared with conventional systems [4].

Chitosan as linear polysaccharides obtained from alkaline deacetylation of chitin is a promising good and applicable biopolymer [5]. Chitosan is insoluble in usual solvent, but chitosan because of their amino groups is soluble in some acid solutions with a pH value lower than 6. It has an excellent film-forming capability and high antimicrobial activity and can be employed as an active antimicrobial coating agent or packaging film [6]. Whey protein isolate (WPI) is another biopolymer with good film-making

capacity isolated from the by-products of cheese-making industries and has interesting mechanical properties [3]. In addition, films formed from whey protein have a transparent appearance and act as excellent gases barriers, but they do not exhibit any antimicrobial properties and do not have good moisture barrier properties unlike the films made of chitosan [7]. Therefore, composed films of whey proteins and chitosan have been developed to overcome these challenges and in order to combine the advantage of each component to film preparation with excellent characterization [8]. However, it was reported that the composite film from whey protein/chitosan had a poor efficiency in physical, mechanical, and permeability properties due to the incompatibility of both ingredients. A promising option to amend the compatibility problems between two polymers is to merge the nanoparticles (NPs) [9].

Titanium dioxide nanoparticles (TiO_2 NP_S) as metal oxides are usually used to improve the attributes of biopolymeric edible films [10]. TiO_2 is a cheap, inert, and safe compound which is extensively applied as an antiradiation and antimicrobial agent because of its photocatalytic properties in the edible films [11]. Furthermore, with respect to the proposed safe dosage, it is extensively applied in cosmetic and food industries to block light and create a white color [10]. Moreover, it was reported that, when a composite matrix was reinforced with TiO_2 NPs, the mechanical properties of the resulting biodegradable samples were significantly increased and the gas barrier and vapor permeability were also reduced [12]. In addition, the addition of TiO_2 NPs to the composite sample causes a decrease in the transmittance light and it is a suitable way to reduce the oxidation of lipid by light [13].

On the other hand, interest in using essential oils in the packaging films has been increased to prevent the chemical deterioration of the packaged foods due to the microbial contamination. Essential oils (EOs) are extracted from the aromatic herbal and are extensively used in food flavoring [14]. The active ingredients in EOs are terpenes, terpenoids, and aromatic ingredients having different antifungal, antiviral, antioxidant, and antibacterial properties. Among all essential oils, *Zataria multiflora* (ZEO) is well known due to antimicrobial properties. It has high-phenolic ingredients, such as carvacrol and thymol [15].

Therefore, it seems that the ZEO and TiO_2 NPs can be used as functional ingredients to enrich edible films based on whey proteins-chitosan owing to their different advantages such antimicrobial activity, nontoxicity, availability, biocompatibility, biodegradability, and good functional properties. The resulting enriched edible films also can be considered as excellent candidates for packaging of food products specially those which are prone to microbial growth to maintain their quality. The overall aim of the current research is to fabricate an edible film made of chitosan and whey proteins enriched with ZEO and TiO_2 NPs for producing biofunctional films with improved biological and functional properties. Subsequently, the antimicrobial, physical, structural, morphological, and mechanical properties of the resulting WPI/chitosan edible film incorporated with TiO_2 NPs and ZEO were studied.

2. Materials and Methods

2.1. Materials. Chitosan, WPI (higher than 91% protein), ZEO, TiO_2 NPs, and glycerol were from Bio Basic (Canada), Hilmar Canada, Barij-Essence Co. (Iran), Acros Co. (USA), and Merck Co. (Darmstadt, Germany), respectively. Also, some materials applied in our research were also from Merck with an analytical grade.

2.2. Composite Film Preparation. Whey protein suspension (3%, w/v) was made by dispersing WPI in DDW subsequently heated at 90°C for 30 min at a pH value of 8.0 and then cooled rapidly [5]. Chitosan solution (10 g/L) was made using dispersing chitosan in 2% (v/v) acetic acid solution by constant mixing for 3 h at 60°C [16]. Based on preliminary experiments, whey protein-chitosan suspension was made by blending two polymer suspensions at a constant ratio of WPI/chitosan (70 : 30) and mixing magnetically for 15 min at 25°C. In the next step, TiO_2 NPs (1 and 2% w/w) were incorporated, and after mixing for 15 min, glycerol (30% w/w) was incorporated to the composite suspension and again stirred for 30 min. Next, ZEO (1% v/v) was incorporated into the composites suspension and sonicated for 30 min with a power of 100 W. For degassing the film suspension, it was placed under vacuum for 20 min. The film suspension was cast onto the Petri dish and dried at 45°C for 24 h. The resulting dried samples were peeled and equilibrated for 2 days in a desiccator with saturated magnesium nitrate solution (RH: 53% at 25°C) until further tests [7].

2.3. Scanning Electron Microscopy (SEM). The morphology of composite WPI/chitosan samples was imaged by a SEM (VEGA II-550, TESCAN, Czech Republic) with an acceleration voltage of 10 kV. Before testing, samples were cut manually in liquid nitrogen. The specimens were stuck onto a stub by tape and sputter-coated by a thin layer of gold. Subsequently, the samples were placed into the SEM chamber and observed with a magnification of 1000x (cross section) and 5000× (surface area) [17].

2.4. X-Ray Diffraction (XRD). XRD patterns of composite sample, TiO_2 NPs, chitosan, and WPI powder samples were recorded with the X-ray diffractometer (Philips PW1730, PANalytical, Netherlands) using the Cu Kα radiation source (40 kV and 30 mA). The analysis was done in the 2θ range between 10° and 50° [18].

2.5. Fourier-Transform Infrared (FTIR) Spectroscopy. Composite WPI/chitosan sample FTIR spectroscopy was performed by a Bruker infrared spectrometer (Billerica, Massachusetts, USA) to evaluate the influence of addition of TiO_2 NPs and ZEO. The wavenumber region of samples mixed with potassium bromide was evaluated at 4000–600 cm^{-1} with 4 cm^{-1} interval [1].

2.6. Thickness of Films. Thickness was determined using a manual micrometer with a precision of 1 μm. Ten different locations of samples were measured, and the average was taken as the result [19].

2.7. Swelling Ratio. The composite film pieces of 20×20 mm in size were dried in an oven at 104°C, weighed, (W_i) and then immersed in 50 mL DDW at room temperature for 24 h. Excess liquid on the wet films were removed by the filter paper and weighed (W_f). The capacity of water absorption was determined according to the following equation:

$$\text{swelling ratio}\,(\%) = \frac{w_f - w_i}{w_i} \times 100. \quad (1)$$

2.8. Water Vapor Permeability. Water vapor permeability of samples was determined gravimetrically based on the technique of Jiang et al. [20]. A circular cup was filled with DDW to expose the lower film face to provide RH of 100%. Composite films were mounted with adhesives on the cups and then were maintained in a desiccator containing the saturation $MgNo_3$ solution ($53 \pm 2\%$ RH) at 25°C. The cup weight loss was determined every 1 h to 8 h to measure the line slope of the mass loss (g) against time (s). The WVP of the samples was calculated by

$$\text{WVP}\left(\text{g} \cdot \text{m}^{-1} \cdot \text{s}^{-1} \cdot \text{kPa}^{-1}\right) = \frac{M \times T}{A \times \Delta P}, \quad (2)$$

where M is the linear portion (g/s), T is the sample thickness (m), A is the area of exposed film (m^2), and ΔP is the partial pressure difference of water vapor across the sample (kPa).

2.9. Mechanical Properties. Mechanical properties including tensile strength (TS) and elongation at break (EAB) of each composite sample were analyzed with a texture analyzer instrument (Testometric Co., Ltd., England). Rectangular piece samples ($1.6 \times 6\ cm^2$) were kept at an ambient temperature ($53 \pm 2\%$ RH) for 48 h. The sample specimens were mounted between the grips adjusted to 3 cm distance separation and then stretched with 83.33 mm/s. Mechanical properties were carried out with 6 replications [19].

2.10. Optical Characterization. The color indexes of samples evaluated by using a Minolta colorimeter (CR-300, Japan). L^* (lightness), a^* (green-red), and b^* (blue-yellow) were evaluated on the samples. In addition, the samples opacity were determined with placing directly the film specimens in the spectrophotometer, and their absorption was read at the 600 nm with an empty test cell as the reference using an UV-VIS spectrophotometer. Opacity of the composite samples was determined as follows:

$$\text{opacity} = \frac{A_{600}}{x}, \quad (3)$$

where x is the film thickness (mm) [21].

2.11. Antimicrobial Properties. Antimicrobial properties of composite films were measured by the disc diffusion technique. Three kinds of microorganisms including *Listeria monocytogenes*, *Escherichia coli*, and *Staphylococcus aureus* were incubated in the nutrient broth media at 37°C overnight. A portion of 100 μL of each microorganism suspension containing 10^7-10^8 cfu/mL of the bacteria was spread in nutrient agar plate surfaces. Afterward, square pieces of the different composite films ($10 \times 10\ mm^2$) were placed on the inoculated agar plate surfaces and kept at 37°C for overnight. The inhibition zone surrounding samples was determined [22].

2.12. Statistical Analysis. SPSS v.16.0 (IBM Software, NY, USA) was applied to study the resulting data. Findings were first evaluated by using one-way analysis of variance (ANOVA), and then the Duncan post hoc test was used to indicate significant ($p < 0.05$) differences between mean film samples.

3. Results and Discussion

3.1. Film Morphology. The composite samples morphology is an important feature because it can ultimately determine the mechanical and physical characteristics of degradable packaging samples [21]. The morphology and microstructure of surface and cross section of the film samples are presented in Figure 1. In the control WPI/chitosan composite sample, some obvious agglomerates were observed in the sample surface due to the heterogeneous structure formation. Our finding was in agreement with the results of Zhang et al. [5] who evaluated the microstructure of chitosan/WPI films enriched by TiO_2 nanoparticles containing sodium laurate. They reported that the blend film made of chitosan and WPI had a ragged and rough surface attributing to the thermodynamic incompatibility and phase segregation of biopolymers. The SEM image shows that TiO_2 NPs and ZEO incorporation into the composite films had no significant influence on the surface morphology of WPI/chitosan samples. In agreement, Zolfi et al. [23] also showed that the surface morphology of kefiran-WPI sample had not been significantly changed by adding of TiO_2 nanoparticle at low concentrations indicating that good dispersion of nanoparticles can be obtained when the content of the particles is very low. However, in our study, some TiO2 particles were visualized on the composite film containing TiO_2 NPs with or without ZEO which can be due to the heterogeneous mixing resulting in agglomerate formation on the film sample surface. The cross-sectional images of all composite samples show smooth and continuous structure. The same observation has been stated for chitosan/TiO_2 nanocomposite films by the Siripatrawan and Kaewklin [24]. Also, the cross-sectional images showed that the composite films had some air bubbles in their cross sections which increased with the addition of ZEO to the composite films. These air bubbles can affect the barrier properties of the resulting films.

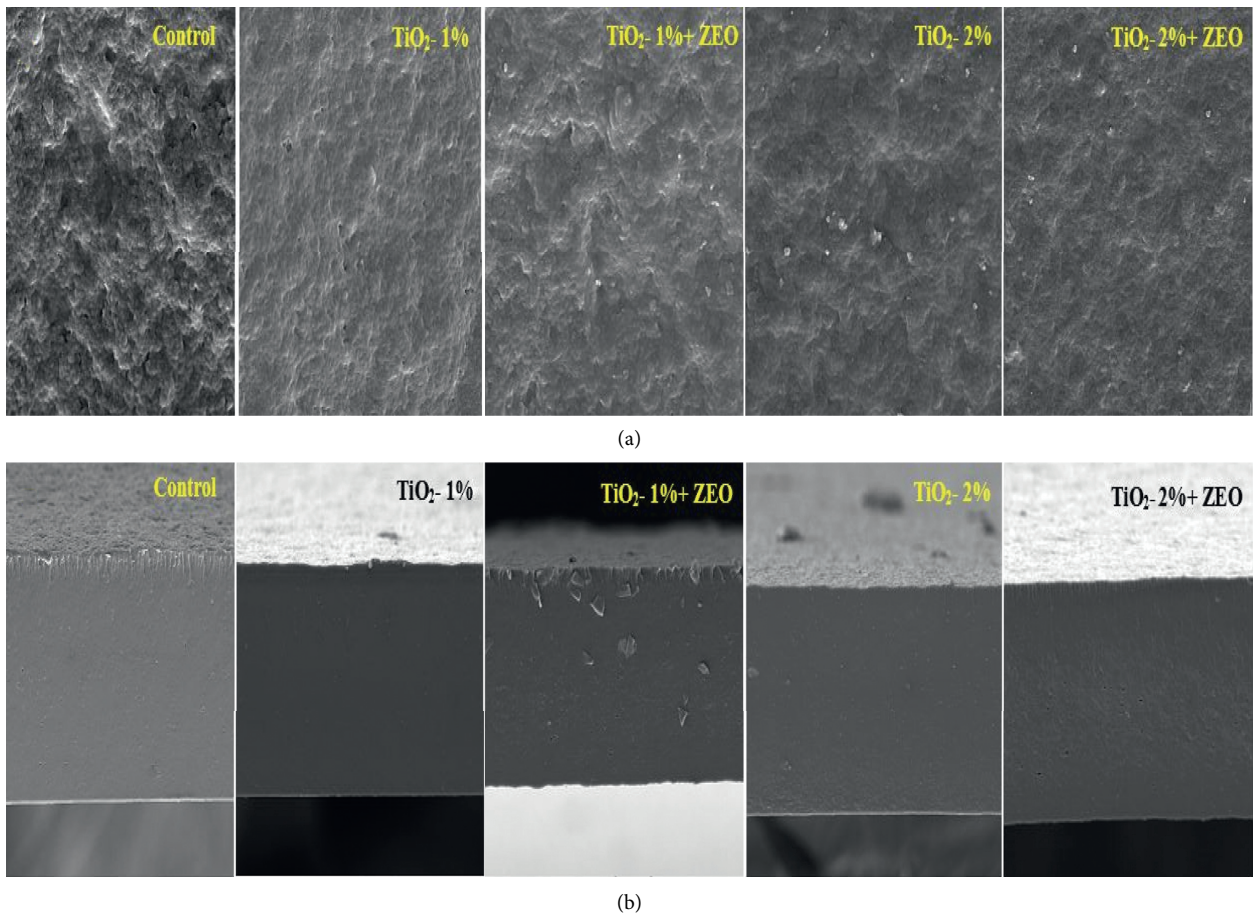

Figure 1: SEM graphs of surface (a) and cross-section (b) of WPI/chitosan samples (control) containing various amounts of TiO_2 (TiO_2-1% and TiO_2-2%) and combination of TiO_2 with ZEO (TiO_2-1% + ZEO and TiO_2-2% + ZEO).

3.2. XRD Pattern. In Figure 2, the XRD graphs of the films are shown. The XRD pattern of TiO_2 NPs showed the significant peaks at $2\theta = 25.69^\circ$, 27.84°, 36.44°, 37.29°, 38.24°, 39.04°, 48.49°, 54.34°, 55.54°, 63.09°, 69.34°, 70.69°, 75.44°, and 76.34° corresponding to the presence of different crystalline phases (anatase and rutile) in the TiO_2 NP structure. The characteristic peak of chitosan appears at 20.59°, which is the typical fingerprint for chitosan [25]. In contrast, WPI displayed an amorphous structure. Results of the formation of composite film between chitosan and WPI showed that the film has an amorphous pattern. This phenomenon can be explained with the modification of chitosan structure due to the amorphous complex formation because it has been reported that proteins are capable of changing the physical state of the chitosan film [2, 5]. When 1% of TiO_2 NP was incorporated in the composite film, two characteristic peaks appeared at 2θ of 21.89° and 25.64°. Addition of 1% ZEO into these composite films caused an inconsiderable shift at the displayed crystalline peak in the film containing 1% TiO_2 NPs at 20.59° and 25.59°, respectively. In accordance with this observation, Oleyaei et al. [11] stated that the appeared peak at around 20° could not be attributed to the TiO_2 NP crystalline phases (anatase or rutile), but it may rather be a good indicator of TiO_2 NP dispersion in the composite sample matrix. Raising TiO2 NP amount to 2%, the XRD pattern of composite films exhibited that the narrow peak intensity at around 25.64° increased and characteristic peak around 20° disappeared. Furthermore, two new signals appeared at the diffraction peak at 2θ of 38.14° and 48.54°. By incorporation of 1% ZEO at these composites film, no significant effect on peak angles at 25.64° and 48.54°, whereas after addition of ZEO in the composite film containing 2% TiO_2 NPs, peaks that appeared at 38.14° disappeared. The diffraction peaks that appeared at $2\theta = 25.64^\circ$, 25.59°, 25.69°, 38.14°, and 48.54° were ascribed to the anatase crystalline of TiO_2 NPs in the composite films with or without ZEO [5, 13]. The results were consistent with the findings of Li et al. [26] and Salarbashi et al. [12] who studied that the crystallinity of the WPI and soluble soybean polysaccharide (SSPS) samples, respectively, increased by TiO_2 NP incorporation.

3.3. FTIR Results. The FTIR results of samples were analysed to identify the interactions between WPI/chitosan, TiO_2 NPs (1 and 2%), and ZEO. The resulting spectra are depicted in Figure 3. The peaks situated at the wavenumbers of 857, 1038, 1155, 1401, 1454, 1538, 1631, and 3273 cm^{-1} were found in all composite films. The characteristic absorption peaks at 857, 1038, and 1155 cm^{-1} attributed to the C-H shaking vibration, N-C bond amide groups, and C-O-C stretching vibration bonds,

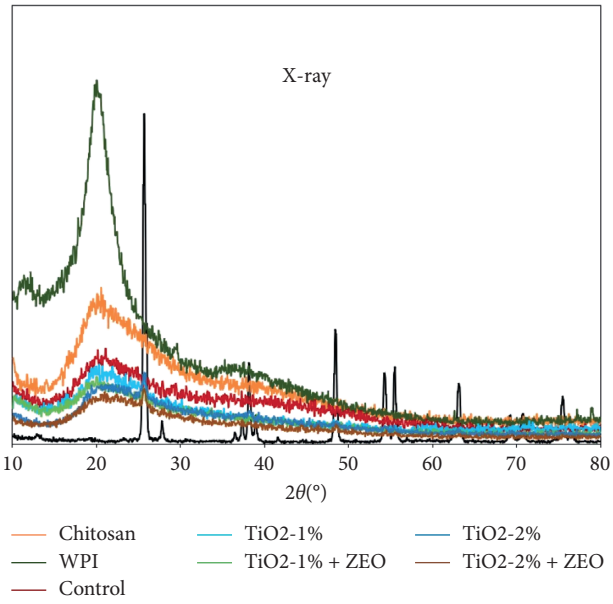

Figure 2: X-ray patterns of WPI/chitosan samples (control) containing various amounts of TiO_2 (TiO_2-1% and TiO_2-2%) and combination of TiO_2 with ZEO (TiO_2-1% + ZEO and TiO_2-2% + ZEO).

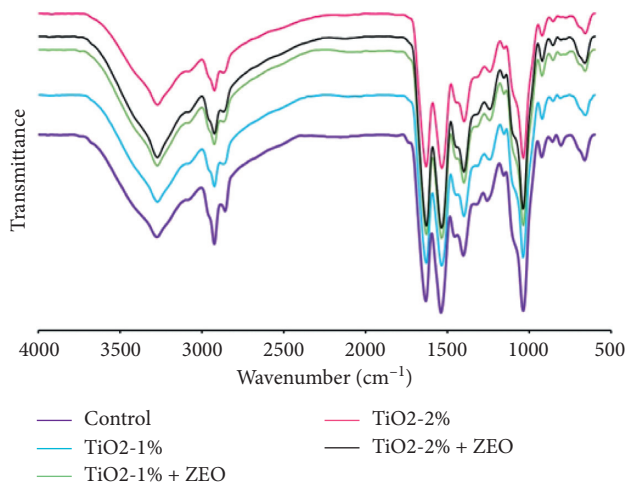

Figure 3: FTIR spectra of WPI/chitosan samples (control) containing various amounts of TiO_2 (TiO_2-1% and TiO_2-2%) and combination of TiO_2 with ZEO (TiO_2-1% + ZEO and TiO_2-2% + ZEO).

respectively [1]. The peaks around 1401 cm^{-1} and 1454 cm^{-1} could be related to the bending vibrations of C-H groups [12], but the main absorption broad peaks at 1631 cm^{-1} and 1538 cm^{-1} refer to the C = O and N-H bending with C-N stretching vibrations at the amide groups of composite film components, respectively, consistent with the existing literature [27]. Additionally, the other peak that appeared at 3273 cm^{-1} was assigned to the hydroxyl (-OH) group vibrations of WPI/chitosan, ZEO, and TiO_2 NPs. After the incorporation of TiO_2 NPs, some observable changes were observed in the composite films. The peaks observed at 804 cm^{-1} in control film disappeared after addition of TiO_2 NPs. Moreover, the band at around 666 cm^{-1} regions with incorporation of 1% and 2% TiO_2 NPs into composite films matrix shifted to ~660 cm^{-1}, indicating the bending vibration of Ti-O-Ti. It is because of hydrogen bond formation between -OH groups of WPI/chitosan and Ti from TiO_2 NPs [24]. Similar results were obtained for TiO_2 NPs with the addition of these NPs in the sample by Kaewklin et al. [28]. The peak situated at 1256 cm^{-1} is due to the vibrations in the plane of C-N and N-H groups of bound amides (amide III) or vibrations of CH_2 groups of glycerol [29]. The blue shift to the wavenumber of 1244 cm^{-1} occurred when TiO_2 NPs (1 and 2%) were added; this might be because of hydrogen bonding formation between functional N-H groups of WPI, chitosan, and -OH groups on the surface of the TiO_2 NPs [1]. Similarly, Arfat et al. [30] observed that the incorporation of ZnO NPs into the fish protein isolate/fish skin gelatin-based composite films caused the blue shift at amide bands to a lower wavelength. Furthermore, observed peaks at a wavenumber around 2923 cm^{-1} and 2857 cm^{-1} in the WPI/chitosan film sample mainly stemmed from the asymmetrical -CH_3 and symmetrical -CH_2 stretching vibrations, respectively [17]. Incorporation of 1 and 2% TiO_2 NPs at the composite films led to small red shift to 2925 cm^{-1} at the methylene groups and also considerably changed to 2871 cm^{-1} at -CH_2 groups, which belongs to the strong hydrophobic interactions in composite films. The major chemical groups in the essential oils are aldehyde, ketone, esters, and phenolic groups [31]. The findings showed that the addition of ZEO had no significant influence on the functional groups related to these compounds in the composite films structure containing 1 and 2% TiO_2 NPs. This can be due to the physical covering and entrapment of the functional groups of ZEO by the functional groups of WPI/chitosan and TiO_2 NPs, and some special interactions were able to remain in the network of the composite films. In fact, it seems that the entrapment of ZEO in the film matrix limited its stretching and bending vibrations; therefore, no significant effect was observed in the FTIR spectra when ZEO was added to the film samples. However, our results were not in line with the findings of Alizadeh-Sani et al. [1] and Ghadetaj et al. [32] who reported that the addition of rosemary and *grammosciadium ptrocarpum* essential oils, respectively, into the matrix of WPI/cellulose nanofibers and WPI films caused a significant change in the functional groups related to hydrophobic interactions and hydrogen bonds. This observed inconsistency in the results can be due to the differences in the biopolymers used to prepare the film samples as well as differences in the composition of EOs.

3.4. Color and Opacity Properties. The visual appearance of biopolymeric films is an important factor in overall acceptance by consumers [3]. The values of opacity, lightness (L^*), green-red (a^*), and blue-yellow (b^*) parameters of composite films are listed in Table 1. The films containing

Table 1: Thickness, swelling ratio, water vapor permeability (WVP), tensile strength (TS), elongation at break (EAB), and optical properties of WPI/chitosan samples containing TiO_2 and TiO_2-ZEO.

Films	Thickness (μmm)	Swelling ratio (%)	WVP (10^{-10} g·m MPa^{-1}s^{-1}·m^{-2})	TS (MPa)	EAB (%)	Color			Opacity
						L^*	a^*	b^*	
Control	66.93 ± 1.23^{b}	65.08 ± 1.62^{e}	3.47 ± 0.07^{b}	6.03 ± 0.22^{e}	22.37 ± 1.19^{a}	75.1 ± 0.67^{c}	-5.94 ± 0.1^{a}	11.25 ± 0.76^{a}	4.22 ± 0.01^{a}
TiO_2-1%	64.37 ± 1.14^{a}	46.56 ± 0.94^{d}	3.34 ± 0.059^{a}	8.80 ± 0.83^{b}	17.39 ± 0.99^{b}	90.45 ± 0.75^{b}	-5.79 ± 0.47^{ab}	13.63 ± 0.24^{b}	12.50 ± 0.04^{b}
TiO_2-1% + ZEO	71.31 ± 1.13^{c}	17.59 ± 1.30^{b}	3.70 ± 0.058^{c}	8.14 ± 0.45^{d}	13.62 ± 1.19^{c}	86.51 ± 0.48^{d}	-5.13 ± 0.16^{ab}	13.94 ± 0.36^{b}	14.24 ± 0.01^{c}
TiO_2-2%	66.81 ± 1.22^{b}	35.79 ± 1.29^{c}	3.47 ± 0.063^{b}	9.44 ± 0.48^{a}	12.88 ± 1.34^{d}	92.02 ± 0.71^{a}	-4.78 ± 0.61^{b}	13.55 ± 0.62^{b}	21.40 ± 0.05^{d}
TiO_2-2% + ZEO	73.50 ± 1.21^{d}	12.12 ± 1.00^{a}	3.81 ± 0.084^{d}	8.71 ± 0.56^{c}	11.28 ± 1.70^{d}	88.75 ± 0.79^{c}	-4.87 ± 0.78^{ab}	16.02 ± 0.63^{c}	22.15 ± 0.10^{e}

Data are shown as average ± standard deviation. Different letters in the same column show significant differences ($p < 0.05$).

TiO_2 NPs and a combination of TiO_2 NPs and ZEO presented significant differences in the case of all color parameters and values of opacity in comparison with the control sample. The composite films containing 1% and 2% TiO_2 NPs showed a considerable increase in b^* and a slight decrease in a^*. The lightness or whiteness of samples with the addition of TiO_2 NPs went up significantly ($p < 0.05$) from 75.1 to 92.02. The ZEO incorporation in the TiO_2-containing composite films caused a slight reduction in the lightness and an increase in the yellowness and the tendency of the film redness. On the other hand, the transmittance results at 600 nm presented that the control film had the highest transparency, whereas the transparency of composite films containing TiO_2 NPs considerably decreased and also there was an increase in the TiO_2 NP amount from 1% to 2%. The transparency of composite biopolymer films significantly decreased. Also, the ZEO combination had a significant influence on the TiO_2-composite sample opacity causing a decrease in the transparency of the films. In agreement with these findings, Hosseini et al. [33] showed that the reduction of film transparency with the incorporation of nanoparticles could be because of their aggregation which can block the light transmission. These results were in harmony with the findings reported on the incorporation of TiO_2 NPs to WPI/chitosan [5] and gelatin/agar films [13]. Similarly, it has been reported that the hake protein film transparency reduced after compounding with thyme EO [34].

3.5. Swelling Ratio. The swelling ratio is an important factor in composite films and represents its water absorption resistance property and type of film use [35]. Table 1 exhibits the swelling ratio of different composite films. As seen, the control presented the highest swelling ratio (65.08%). A significant decrease in the swelling ratio was exhibited for composite samples with the addition of 1 and 2% TiO_2 NPs and reached to 46.56% and 35.79%, respectively. A similar trend obtained by Achachlouei and Zahedi [9] showed that the water absorption of CMC films considerably reduced after combination with TiO_2 NPs. This result can be due to the hydrogen bond formation among WPI/chitosan, glycerol, and TiO_2 NPs which decreased the hydrophilic groups on the sample matrix and free space of the network to water molecule diffusion inside the films [13]. In addition, it has been suggested that the reduction in water uptake can be because of the hydrophobic nature of TiO_2 NPs [11]. In contrast, Ren et al. [36] presented that the water-binding capacity of PVA/xylan samples went up by TiO_2 NPs incorporation, and the film containing the highest amount of rutile TiO_2 NPs showed the highest swelling ratio. On the other hand, the results of the addition of the ZEO into the composite film formulation containing 1 and 2% TiO_2 NPs demonstrated that the swelling ratio of films significantly reduced to 17.59% and 12.12%, respectively. This phenomenon is due to the ZEO hydrophobic nature that caused an increase in the hydrophobicity of the composite-TiO_2 NPs films, which caused a lower affinity of samples to water [37]. It was also reported that the sample swelling ratio was altered by adding rosemary and mint essential oils and then decreased [35]. Thereby, it can be concluded that that the incorporation of TiO_2 NPs and essential oil into the composite films can improve the usability of films for high-humidity food packaging.

3.6. Composite Film Thickness and WVP. The thickness can be changed by the inclusion of ingredients to the blend film. The water vapor transfer is one the most important characteristics of food packaging polymer films. Low vapor permeability that reduces the transfer of moisture between the outer atmosphere and the food environment is a determining factor of the application of film produced in food packaging [35]. In general, similar findings were shown for both the thickness and WVP of composite samples by incorporation of TiO_2 NPs and ZEO. The findings showed that the average thickness and WVP of composite films were between 0.064 and 0.073 mm and 3.34 and 3.81×10^{-10} g·s^{-1}·m^{-1}·kPa, respectively (Table 1). The thickness and WVP of control composite film were 0.066 mm and 3.47×10^{-10} g·s^{-1}·m^{-1}·kPa, respectively, and inclusion of 1% TiO_2 into composite film matrix caused a remarkable ($p < 0.05$) effect on this parameter of composite films and reduced to a lower amount. Nevertheless, the increase in TiO_2 NP concentration from 1 to 2% had no effects on the thickness and WVP of composite samples in comparison with the control film. This can be because of the proper dispersion of the nanoparticles at lower concentrations, which, in addition to forming a compact structure and reducing the thickness, also blocks the water vapor entry [38]. It has been shown that the thickness of the WPI film significantly increased after loading 1.5% TiO_2 NPs into the WPI matrix which was inconsistent with our findings [1]. However, Vejdan et al. [13] about WVP decrease in the samples containing NPs theoretically stated that this could be attributed mostly to the tortuous path introduced by impermeable TiO2 NPs distributed in the matrix, in which water molecules permeate forcing to the increase of the transmission length. The positive effects of TiO_2 NPs on WVP of some polymers such as wheat gluten/nanocellulose [39], kefiran/WPI [23], and pectin [40] have been revealed in different investigations.

Furthermore, the incorporation of ZEO into the composite films containing 1 and 2% TiO_2 NPs caused a significant increase in the average thickness to 0.071 and 0.073 mm and WVP of composite films to 3.70 and 3.81×10^{-10} g·s^{-1}·m^{-1}·kPa, respectively. These results are in accordance with results of summer savory essential oil (SSEO) into the blend carboxymethyl cellulose-agar film [41]. Increase in the WVP of samples followed by loading ZEO in fact can be because of the negative effect of the essential oils on the intermolecular bonding thus creating the free spaces between the chains and phase separation due to matrix incompatibility and presence of water molecules throughout the network of the composite film [32]. The findings of our research are in agreement with data reports on WVP of essential oil-incorporated films [32, 42]. Also, the data of this study are in contrast with those in the article by Shojaei-Aliabadi et al. [15] and Nisar et al. [43] which reported that the lower WVP was

Table 2: The antimicrobial activity of WPI/chitosan samples incorporated with TiO_2 and TiO_2-ZEO.

Films	Diameter of inhibition zone (mm)		
	L. monocytogenes (Gram +)	*S. aureus* (Gram +)	*E. coli* (Gram −)
Control	0.00 ± 0.00^{c}	0.00 ± 0.00^{c}	0.00 ± 0.00^{c}
TiO_2-1%	0.00 ± 0.00^{c}	0.00 ± 0.00^{c}	0.00 ± 0.00^{c}
TiO_2-1% + ZEO	7.90 ± 1.20^{b}	14.0 ± 2.00^{b}	8.2 ± 1.30^{b}
TiO_2-2%	0.00 ± 0.00^{c}	0.00 ± 0.00^{c}	0.00 ± 0.00^{c}
TiO_2-2% + ZEO	8.50 ± 1.00^{a}	23.20 ± 3.20^{a}	9.50 ± 1.50^{a}

Data are shown as average ± standard deviation. Different letters in the same column show significant differences ($p < 0.05$).

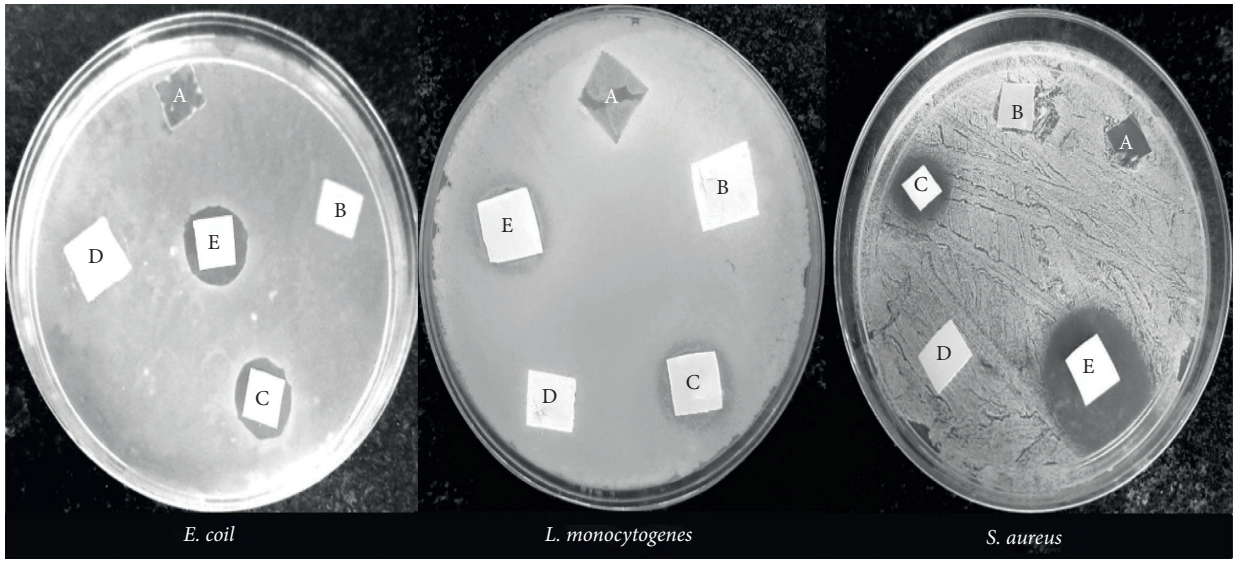

Figure 4: Antimicrobial activity of different composite films: control (A), containing 1% TiO_2 (B), 1% TiO_2 with ZEO (C), 2% TiO_2 (D), and 2% TiO_2 with ZEO (E) against three types of study bacteria.

obtained with formulation of ZEO oil into the kappa-carrageenan/nanoclay composite film and clove bud essential oil at the pectin film, respectively.

3.7. Mechanical Properties of Composite Films. The influences of TiO2 NPs and ZEO on the mechanical characterization of samples including TS and EAB are shown in Table 1. Compared with the control film, the incorporation of TiO2 NPs caused a significant ($p < 0.05$) increase in the TS values of composite films. Results indicated that the control film had a TS of 6.06 MPa with the loading of 1 and 2% TiO_2 NPs; the TS values considerably increased to 8.80 and 9.44 MPa, respectively. However, the addition of ZEO into the matrix of blends film containing 1 and 2% TiO_2 NPs led to a significant decrease at the resistance of the composite film to 8.14 and 8.71 MPa, respectively. In contrary to the TS, a drastic decrease from 22.37% to 17.32% and 12.88%, respectively, occurred because of the flexibility of the composite films with inclusions of 1 and 2% TiO_2 NPs. Hence, the addition of ZEO to the composite film containing 1% TiO_2 NPs remarkably reduced the EAB of film to 13.62%, while the incorporation of ZEO to the film matrix at a concentration of 2% TiO_2 NPs had an insignificant influence on the elongation capacity of sample (11.28%). The increase in strength and decrease in the flexibility of the composite films by TiO2 NPs addition can be because of the uniform distribution of TiO2 NPs through interfacial interactions such as electrostatic interactions, hydrogen bonds, and O-Ti-O bonds with other compounds in the film, consequently increasing the cohesion force of the film causes a restriction of the motion of polymeric network [29, 39]. These results coincide with the incorporation of TiO_2 NPs into soluble soybean polysaccharide [44] and starch/pectin film [40]; it was found that the sample TS was increased by the gradual increase of TiO_2 nanoparticles. Further, in contrast with our finding, Siripatrawan and Kaewklin [24] obtained that the tensile resistance of chitosan and TiO_2 nanocomposite films increases when low amounts were incorporated, but decrease in higher TiO_2 NP amount is probably because of the agglomeration of TiO_2 NPs in effect of inhomogeneous dispersion at a certain concentration. But, decrease in the tensile resistance and EAB after addition of ZEO may be because of the weakening of intermolecular connection of the sample by reducing the main interactions and increasing the breakup of film network due to heterogeneous with matrix of composite films, which caused a decrease in the film rigidity and resistance [1]. This result matched with that reported by the previous research about adding summer savory EO to CMC-agar edible composite film [41] or

incorporating cinnamon and ginger essential oils to CMC-chitosan blend samples [45].

3.8. Antimicrobial Properties. Antibacterial properties of films against *L. monocytogenes*, *S. aureus* (Gram-positive), and *E. coli* (Gram-negative) food pathogenic bacteria are illustrated in Table 2 and depicted in Figure 4. Results indicated that control films and films containing 1 and 2% TiO_2 NPs had no antimicrobial activity, whereas TiO_2-containing (1 and 2%) composite films loaded with ZEO had an antimicrobial effect against all pathogenic bacteria. This may be related to the non-UV treatment of the NPs at this study because it has been reported that UV modification significantly increases the functionality of the NPs such as antimicrobial activity. Same findings were previously shown by Ahmadi et al. [46]. But, TiO2 NPs have a synergistic influence on the antimicrobial properties of ZEO; in that way, the film containing the essential oil showed a higher antimicrobial activity when combined with 2% TiO_2 NPs than with 1%, which was evident in the results of the growth inactivation ofall three microbes, especially *S. aureus*. Also, overall, composite films showed a lower microbial inhibition zone against Gram-negative than against the Gram-positive bacteria. This is due to the structural difference in the bacterial cell wall. Gram-negative bacteria have complex cell wall compared with Gram-positive bacteria [47]. In agreement with these findings, some researches showed a higher antimicrobial activity for essential oil and NPs against Gram-positive bacteria in comparison with the Gram-negative ones [14, 15, 48]. It has been reported in various studies that chitosan due to the presence of positive-charge amino groups has the ability to interact with the negatively charged cell wall of microorganisms, which leads to the breakage of the proteinaceous substrate [16, 49]. Hence, the lack of antibacterial activity in chitosan/WPI-based films in this study, regardless of the addition of essential oils, NPs, and a type of chitosan, could be because of the less concentration of chitosan in comparison with WPI in the film matrix, which could not show antimicrobial effects. Generally, the antimicrobial effect of TiO_2 NPs and ZEO was associated with its crystalline structure, shape, and size of the NPs [50] and the presence lipophilic and hydrophobic functional group with phenolic components such as carvacrol and thymol with a stronger antimicrobial activity in ZEO [15, 51, 52]. They can bind to the bacterial membrane by different mechanisms, damaging the microbial membrane and cell wall and finally damaging proteins and DNA, causing the cell death [53].

4. Conclusion

WPI/chitosan films loaded with different concentrations of TiO_2 nanoparticles and ZEO showed excellent potential to be applied for packaging. The nanoparticles were well distributed in the film structure, and the resulting composite films were homogeneous without any phase separation as observed by SEM. The XRD showed that the incorporation of nanoparticles gradually increased the crystalline structure of samples, which may be because of new bond formation between WPI/chitosan matrix and TiO_2 NPs as investigated by FTIR spectroscopy. However, the findings showed that the incorporation of ZEO had a negligible influence on the crystalline nature of the samples containing TiO_2 nanoparticles. The results of the water vapor permeability test showed that the WVP of WPI/chitosan samples decreased when enriched with TiO_2 nanoparticles, whereas the combination of TiO_2 nanoparticles with ZEO caused a significant increase in the WVP of composite samples. The opacity and color characterization of the samples also changed through the enrichment of films with TiO_2 nanoparticles and ZEO. The addition of TiO_2 nanoparticles and particularly TiO_2-ZEO into the film samples resulted in a significant reduce in their swelling ratio. The mechanical attributes (TS and EAB) of WPI/chitosan films were also modified by the addition of TiO_2 nanoparticles and ZEO. The control WPI/chitosan binary sample and samples containing 1 and 2% TiO_2 did not show any antibacterial activity, while composite films containing TiO_2-ZEO had high antimicrobial activity on both types of bacteria. Generally, the results of our research proposed that WPI/chitosan edible films functionalized by TiO_2 particles and ZEO can be considered as promising candidates for use as active packaging materials for food products owing to their useful antimicrobial properties as well as the suitable physicomechanical characteristics.

Data Availability

The data used to support the study are included within the article. Raw data can be acquired from the corresponding author upon reasonable request (hlashkari@gmail.com).

Conflicts of Interest

The authors declare that they have no conflicts of interest.

References

[1] M. Alizadeh-Sani, A. Khezerlou, and A. Ehsani, "Fabrication and characterization of the bionanocomposite film based on whey protein biopolymer loaded with TiO_2 nanoparticles, cellulose nanofibers and rosemary essential oil," *Industrial Crops and Products*, vol. 124, pp. 300–315, 2018.

[2] C. Valenzuela, L. Abugoch, and C. Tapia, "Quinoa protein-chitosan-sunflower oil edible film: mechanical, barrier and structural properties," *LWT-Food Science and Technology*, vol. 50, no. 2, pp. 531–537, 2013.

[3] M. Kurek, S. Galus, and F. Debeaufort, "Surface, mechanical and barrier properties of bio-based composite films based on chitosan and whey protein," *Food Packaging and Shelf Life*, vol. 1, no. 1, pp. 56–67, 2014.

[4] U. Siripatrawan and B. R. Harte, "Physical properties and antioxidant activity of an active film from chitosan incorporated with green tea extract," *Food Hydrocolloids*, vol. 24, no. 8, pp. 770–775, 2010.

[5] W. Zhang, J. Chen, Y. Chen, W. Xia, Y. L. Xiong, and H. Wang, "Enhanced physicochemical properties of chitosan/whey protein isolate composite film by sodium laurate-modified TiO_2 nanoparticles," *Carbohydrate Polymers*, vol. 138, pp. 59–65, 2016.

[6] I. Leceta, P. Guerrero, and K. De la Caba, "Functional properties of chitosan-based films," *Carbohydrate Polymers*, vol. 93, no. 1, pp. 339–346, 2013.

[7] R. Sothornvit, J.-W. Rhim, and S.-I. Hong, "Effect of nanoclay type on the physical and antimicrobial properties of whey protein isolate/clay composite films," *Journal of Food Engineering*, vol. 91, no. 3, pp. 468–473, 2009.

[8] M. Pereda, A. G. Ponce, N. E. Marcovich, R. A. Ruseckaite, and J. F. Martucci, "Chitosan-gelatin composites and bi-layer films with potential antimicrobial activity," *Food Hydrocolloids*, vol. 25, no. 5, pp. 1372–1381, 2011.

[9] B. F. Achachlouei and Y. Zahedi, "Fabrication and characterization of CMC-based nanocomposites reinforced with sodium montmorillonite and TiO_2 nanomaterials," *Carbohydrate Polymers*, vol. 199, pp. 415–425, 2018.

[10] G. Li, S. Park, and B. E. Rittmann, "Developing an efficient TiO_2-coated biofilm carrier for intimate coupling of photocatalysis and biodegradation," *Water Research*, vol. 46, no. 19, pp. 6489–6496, 2012.

[11] S. A. Oleyaei, H. Almasi, B. Ghanbarzadeh, and A. A. Moayedi, "Synergistic reinforcing effect of TiO 2 and montmorillonite on potato starch nanocomposite films: thermal, mechanical and barrier properties," *Carbohydrate Polymers*, vol. 152, pp. 253–262, 2016.

[12] D. Salarbashi, M. Tafaghodi, and B. S. F. Bazzaz, "Soluble soybean polysaccharide/TiO2 bionanocomposite film for food application," *Carbohydrate Polymers*, vol. 186, pp. 384–393, 2018.

[13] A. Vejdan, S. M. Ojagh, A. Adeli, and M. Abdollahi, "Effect of TiO_2 nanoparticles on the physico-mechanical and ultraviolet light barrier properties of fish gelatin/agar bilayer film," *LWT-Food Science and Technology*, vol. 71, pp. 88–95, 2016.

[14] M. Alizadeh-Sani, J.-W. Rhim, M. Azizi-Lalabadi, M. Hemmati-Dinarvand, and A. Ehsani, "Preparation and characterization of functional sodium caseinate/guar gum/TiO_2/cumin essential oil composite film," *International Journal of Biological Macromolecules*, vol. 145, pp. 835–844, 2020.

[15] S. Shojaee-Aliabadi, M. A. Mohammadifar, H. Hosseini et al., "Characterization of nanobiocomposite kappa-carrageenan film with Zataria multiflora essential oil and nanoclay," *International Journal of Biological Macromolecules*, vol. 69, pp. 282–289, 2014.

[16] A. M. Youssef, S. M. El-Sayed, H. S. El-Sayed, H. H. Salama, and A. Dufresne, "Enhancement of Egyptian soft white cheese shelf life using a novel chitosan/carboxymethyl cellulose/zinc oxide bionanocomposite film," *Carbohydrate Polymers*, vol. 151, pp. 9–19, 2016.

[17] L. Qu, G. Chen, S. Dong et al., "Improved mechanical and antimicrobial properties of zein/chitosan films by adding highly dispersed nano-TiO2," *Industrial Crops and Products*, vol. 130, pp. 450–458, 2019.

[18] H. T. Kevij, M. Salami, M. Mohammadian, and M. Khodadadi, "Fabrication and investigation of physicochemical, food simulant release, and antioxidant properties of whey protein isolate-based films activated by loading with curcumin through the pH-driven method," *Food Hydrocolloids*, vol. 108, Article ID 106026, 2020.

[19] M. Moghadam, M. Salami, M. Mohammadian, M. Khodadadi, and Z. Emam-Djomeh, "Development of antioxidant edible films based on mung bean protein enriched with pomegranate peel," *Food Hydrocolloids*, vol. 104, Article ID 105735, 2020.

[20] X. Jiang, H. Li, Y. Luo, Y. Zhao, and L. Hou, "Studies of the plasticizing effect of different hydrophilic inorganic salts on starch/poly (vinyl alcohol) films," *International Journal of Biological Macromolecules*, vol. 82, pp. 223–230, 2016.

[21] Q. Wang, H. Yu, B. Tian et al., "Novel edible coating with antioxidant and antimicrobial activities based on whey protein isolate nanofibrils and carvacrol and its application on fresh-cut cheese," *Coatings*, vol. 9, no. 9, 2019.

[22] Y. Ruiz-Navajas, M. Viuda-Martos, E. Sendra, J. A. Perez-Alvarez, and J. Fernández-López, "In vitro antibacterial and antioxidant properties of chitosan edible films incorporated with Thymus moroderi or Thymus piperella essential oils," *Food Control*, vol. 30, no. 2, pp. 386–392, 2013.

[23] M. Zolfi, F. Khodaiyan, M. Mousavi, and M. Hashemi, "Development and characterization of the kefiran-whey protein isolate-TiO_2 nanocomposite films," *International Journal of Biological Macromolecules*, vol. 65, pp. 340–345, 2014.

[24] U. Siripatrawan and P. Kaewklin, "Fabrication and characterization of chitosan-titanium dioxide nanocomposite film as ethylene scavenging and antimicrobial active food packaging," *Food Hydrocolloids*, vol. 84, pp. 125–134, 2018.

[25] Y. Zhang, X. Zhang, R. Ding, J. Zhang, and J. Liu, "Determination of the degree of deacetylation of chitosan by potentiometric titration preceded by enzymatic pretreatment," *Carbohydrate Polymers*, vol. 83, no. 2, pp. 813–817, 2011.

[26] Y. Li, Y. Jiang, F. Liu, F. Ren, G. Zhao, and X. Leng, "Fabrication and characterization of TiO2/whey protein isolate nanocomposite film," *Food Hydrocolloids*, vol. 25, no. 5, pp. 1098–1104, 2011.

[27] B. Lin, Y. Luo, Z. Teng, B. Zhang, B. Zhou, and Q. Wang, "Development of silver/titanium dioxide/chitosan adipate nanocomposite as an antibacterial coating for fruit storage," *LWT-Food Science and Technology*, vol. 63, no. 2, pp. 1206–1213, 2015.

[28] P. Kaewklin, U. Siripatrawan, A. Suwanagul, and Y. S. Lee, "Active packaging from chitosan-titanium dioxide nanocomposite film for prolonging storage life of tomato fruit," *International Journal of Biological Macromolecules*, vol. 112, pp. 523–529, 2018.

[29] Q. He, Y. Zhang, X. Cai, and S. Wang, "Fabrication of gelatin-TiO2 nanocomposite film and its structural, antibacterial and physical properties," *International Journal of Biological Macromolecules*, vol. 84, pp. 153–160, 2016.

[30] Y. A. Arfat, S. Benjakul, T. Prodpran, P. Sumpavapol, and P. Songtipya, "Properties and antimicrobial activity of fish protein isolate/fish skin gelatin film containing basil leaf essential oil and zinc oxide nanoparticles," *Food Hydrocolloids*, vol. 41, pp. 265–273, 2014.

[31] A. A. Mohamed, G. A. El-Emary, and H. F. Ali, "Influence of some citrus essential oils on cell viability, glutathione-S-transferase and lipid peroxidation in Ehrlich ascites carcinoma cells," *Journal of American Science*, vol. 6, no. 10, pp. 820–826, 2010.

[32] A. Ghadetaj, H. Almasi, and L. Mehryar, "Development and characterization of whey protein isolate active films containing nanoemulsions of Grammosciadium ptrocarpum Bioss. essential oil," *Food Packaging and Shelf Life*, vol. 16, pp. 31–40, 2018.

[33] S. F. Hosseini, M. Rezaei, M. Zandi, and F. Farahmandghavi, "Fabrication of bio-nanocomposite films based on fish gelatin reinforced with chitosan nanoparticles," *Food Hydrocolloids*, vol. 44, pp. 172–182, 2015.

[34] C. Pires, C. Ramos, G. Teixeira et al., "Characterization of biodegradable films prepared with hake proteins and thyme

oil," *Journal of Food Engineering*, vol. 105, no. 3, pp. 422–428, 2011.

[35] R. Akhter, F. A. Masoodi, T. A. Wani, and S. A. Rather, "Functional characterization of biopolymer based composite film: incorporation of natural essential oils and antimicrobial agents," *International Journal of Biological Macromolecules*, vol. 137, pp. 1245–1255, 2019.

[36] J. Ren, S. Wang, C. Gao, X. Chen, W. Li, and F. Peng, "TiO_2-containing PVA/xylan composite films with enhanced mechanical properties, high hydrophobicity and UV shielding performance," *Cellulose*, vol. 22, no. 1, pp. 593–602, 2015.

[37] Y. Peng and Y. Li, "Combined effects of two kinds of essential oils on physical, mechanical and structural properties of chitosan films," *Food Hydrocolloids*, vol. 36, pp. 287–293, 2014.

[38] E. Jamróz, P. Kopel, L. Juszczak et al., "Development of furcellaran-gelatin films with Se-AgNPs as an active packaging system for extension of mini kiwi shelf life," *Food Packaging and Shelf Life*, vol. 21, p. 100339, 2019.

[39] N. A. El-Wakil, E. A. Hassan, R. E. Abou-Zeid, and A. Dufresne, "Development of wheat gluten/nanocellulose/titanium dioxide nanocomposites for active food packaging," *Carbohydrate Polymers*, vol. 124, pp. 337–346, 2015.

[40] K. K. Dash, N. A. Ali, D. Das, and D. Mohanta, "Thorough evaluation of sweet potato starch and lemon-waste pectin based-edible films with nano-titania inclusions for food packaging applications," *International Journal of Biological Macromolecules*, vol. 139, pp. 449–458, 2019.

[41] M. Abdollahi, S. Damirchi, M. Shafafi, M. Rezaei, and P. Ariaii, "Carboxymethyl cellulose-agar biocomposite film activated with summer savory essential oil as an antimicrobial agent," *International Journal of Biological Macromolecules*, vol. 126, pp. 561–568, 2019.

[42] M. Jouki, S. A. Mortazavi, F. T. Yazdi, and A. Koocheki, "Characterization of antioxidant-antibacterial quince seed mucilage films containing thyme essential oil," *Carbohydrate Polymers*, vol. 99, pp. 537–546, 2014.

[43] T. Nisar, Z.-C. Wang, X. Yang, Y. Tian, M. Iqbal, and Y. Guo, "Characterization of citrus pectin films integrated with clove bud essential oil: physical, thermal, barrier, antioxidant and antibacterial properties," *International Journal of Biological Macromolecules*, vol. 106, pp. 670–680, 2018.

[44] T. Shaili, M. N. Abdorreza, and N. Fariborz, "Functional, thermal, and antimicrobial properties of soluble soybean polysaccharide biocomposites reinforced by nano TiO_2," *Carbohydrate Polymers*, vol. 134, pp. 726–731, 2015.

[45] N. Noshirvani, B. Ghanbarzadeh, C. Gardrat et al., "Cinnamon and ginger essential oils to improve antifungal, physical and mechanical properties of chitosan-carboxymethyl cellulose films," *Food Hydrocolloids*, vol. 70, pp. 36–45, 2017.

[46] R. Ahmadi, A. Tanomand, F. Kazeminava et al., "Fabrication and characterization of a titanium dioxide (TiO_2) nanoparticles reinforced bio-nanocomposite containing Miswak (*Salvadora persica* L.) extract–the antimicrobial, thermophysical and barrier properties," *International Journal of Nanomedicine*, vol. 14, pp. 3439–3454, 2019.

[47] X. Tang, J. Dai, H. Sun et al., "Mechanical strength, surface properties, cytocompatibility and antibacterial activity of nano zinc-magnesium silicate/polyetheretherketone biocomposites," *Journal of Nanoscience and Nanotechnology*, vol. 19, no. 12, pp. 7615–7623, 2019.

[48] S. M. Hasheminya, R. R. Mokarram, B. Ghanbarzadeh, H. Hamishekar, H. S. Kafil, and J. Dehghannya, "Development and characterization of biocomposite films made from kefiran, carboxymethyl cellulose and Satureja Khuzestanica essential oil," *Food Chemistry*, vol. 289, pp. 443–452, 2019.

[49] M. P. Indumathi, K. S. Sarojini, and G. R. Rajarajeswari, "Antimicrobial and biodegradable chitosan/cellulose acetate phthalate/ZnO nano composite films with optimal oxygen permeability and hydrophobicity for extending the shelf life of black grape fruits," *International Journal of Biological Macromolecules*, vol. 132, pp. 1112–1120, 2019.

[50] G. Carré, E. Hamon, S. Ennahar et al., "TiO_2 photocatalysis damages lipids and proteins in *Escherichia coli*," *pplied and Environmental Microbiology*, vol. 80, no. 8, pp. 2573–2581, 2014.

[51] A. Dashipour, V. Razavilar, H. Hosseini et al., "Antioxidant and antimicrobial carboxymethyl cellulose films containing Zataria multiflora essential oil," *International Journal of Biological Macromolecules*, vol. 72, pp. 606–613, 2015.

[52] M. Raeisi, F. Ghorbani Bidkorpeh, M. Hashemi et al., "Chemical composition and antibacterial and antioxidant properties of essential oils of *Zataria* multiflora, Artemisia deracunculus and Mentha piperita," *Medical Laboratory Journal*, vol. 13, no. 2, pp. 1–7, 2019.

[53] H. Ando, N. Kawasaki, N. Yamano, K. Uegaki, and A. Nakayama, "Biodegradation of a poly (ε-caprolactone-co-l-lactide)–visible-light-sensitive TiO_2 composite with an on/off biodegradation function," *Polymer Degradation and Stability*, vol. 114, pp. 65–71, 2015.